Electronic Supplementary Information

H_2 and CH_4 Productions from Bio-alcohols by Condensed Poly (Heptazine Imide) with Visible Light

Dandan Zheng,[1] Jingmin Zhou,[1] Zhongpu Fang,[2] Tobias Heil,[3] Aleksandr Savateev,[3] Yongfan Zhang,[2] Markus Antonietti,[3] Guigang Zhang[2,3*] and Xinchen Wang[2*]

[1]College of Environment & safety engineering, Fuzhou University, Fuzhou 350116, China

[2]State Key Laboratory of Photocatalysis on Energy and Environment, College of Chemistry, Fuzhou University, Fuzhou, 350116, China

[3]Department of Colloids Chemistry, Max Planck Institute of Colloids and Interfaces, Research Campus Golm, 14476 Potsdam, Germany

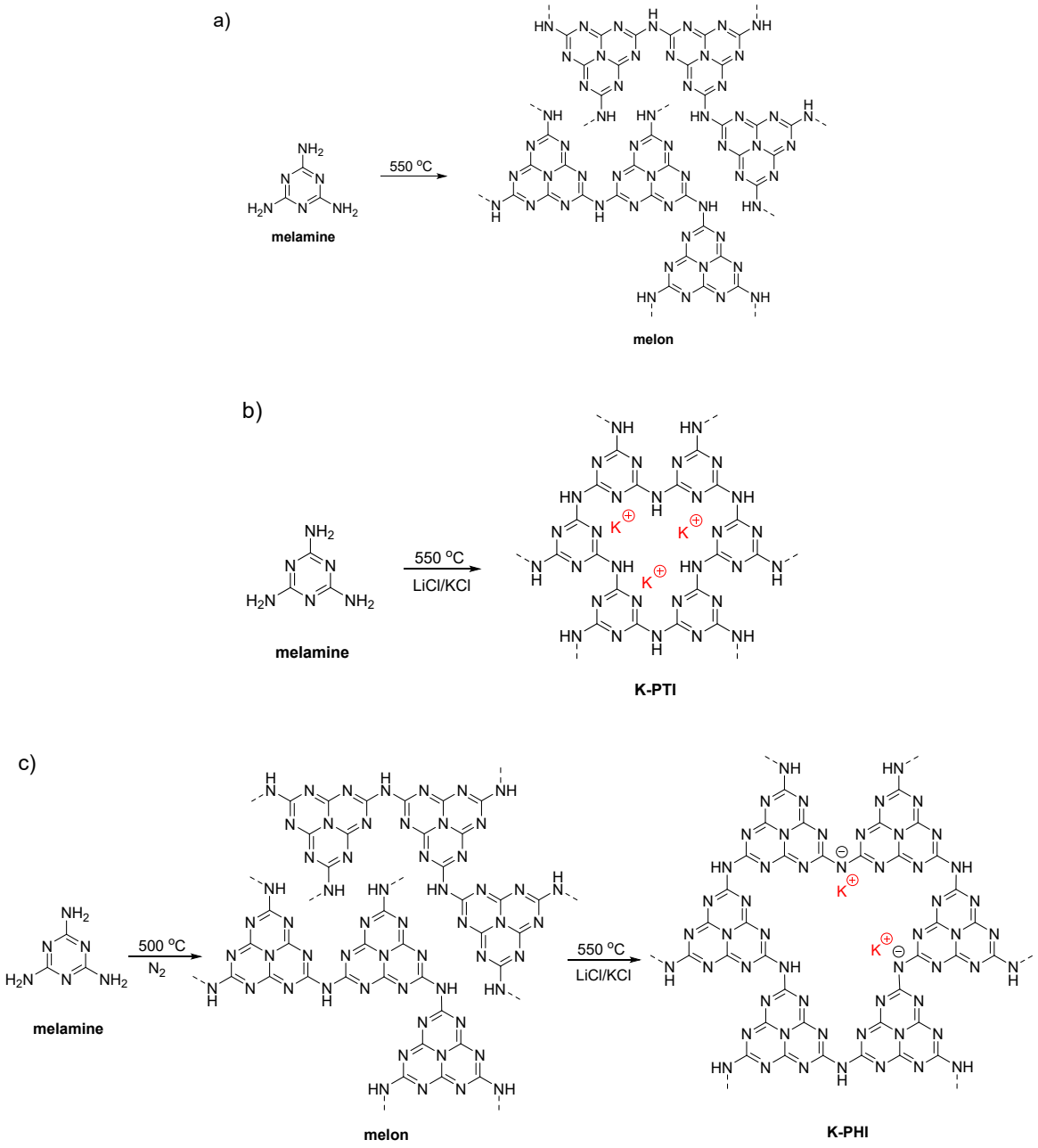

Scheme S1. Proposed formation of (a) melon, (b) K-PTI and (c) K-PHI based carbon nitrides used for photocatalytic H_2 evolution.

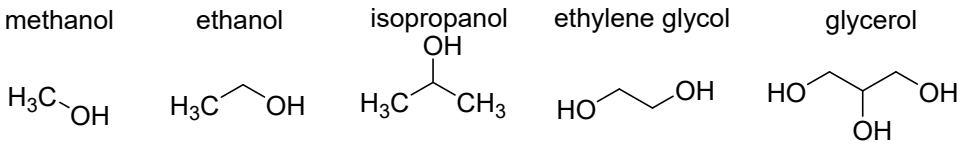

Scheme S2. Molecular structures of the alcohols used for photocatalytic H_2 evolution in this study.

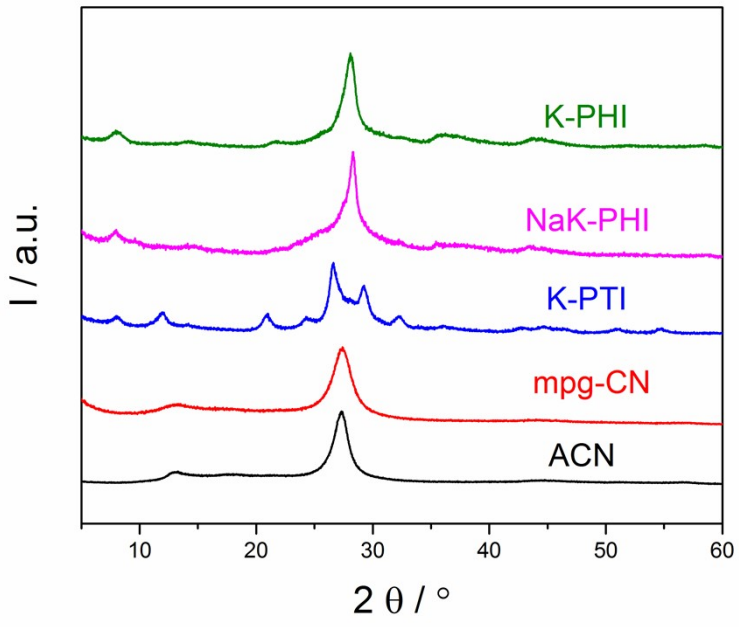

Figure S1. Powder XRD patterns of different CN photocatalysts as investigated for photocatalytic H_2 evolution studies.

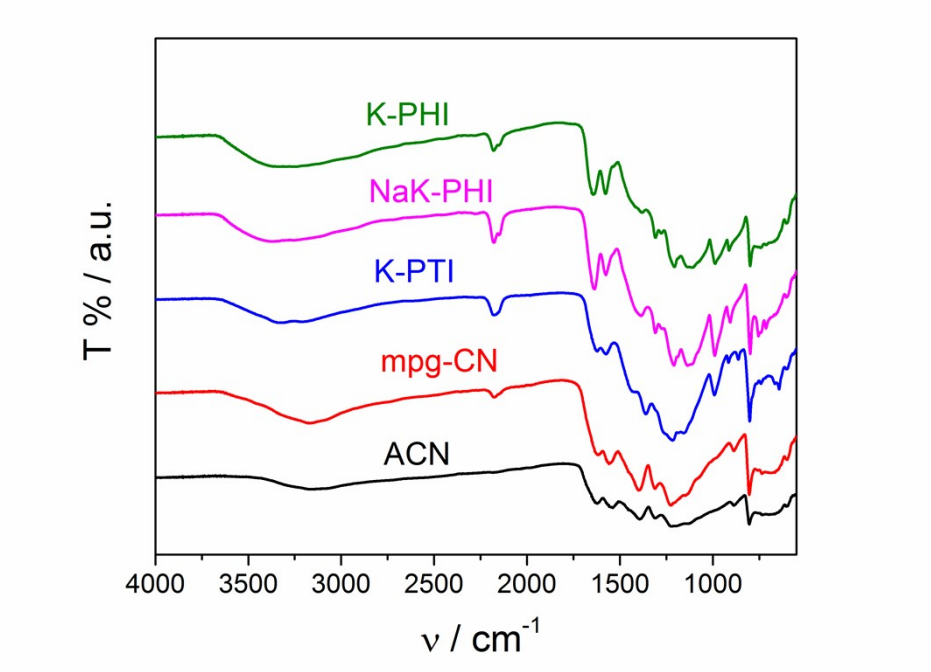

Figure S2. FT-IR of different CN photocatalysts as investigated for photocatalytic H_2 evolution studies.

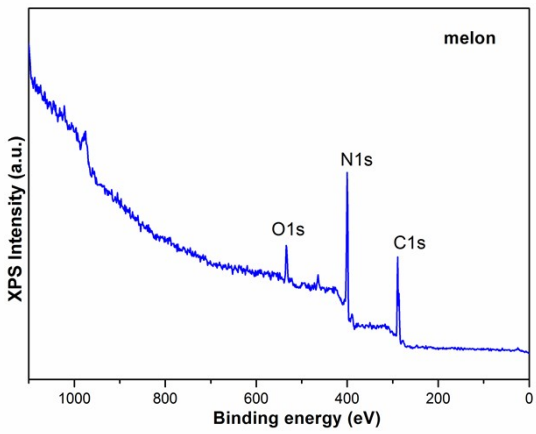
melon
XPS Intensity (a.u.)
O1s
N1s
C1s
1000
800
600
400
200
0
Binding energy (eV)

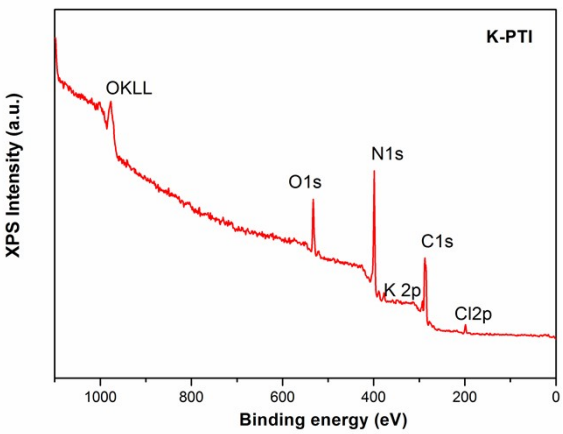
K-PTI
XPS Intensity (a.u.)
OKLL
O1s
N1s
C1s
K 2p
Cl2p
1000
800
600
400
200
0
Binding energy (eV)

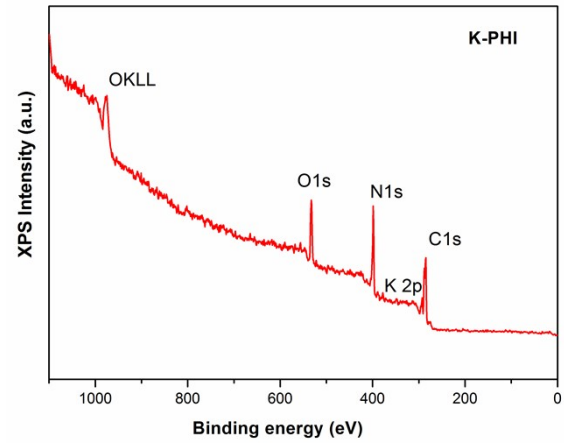
K-PHI
XPS Intensity (a.u.)
OKLL
O1s
N1s
C1s
K 2p
1000
800
600
400
200
0
Binding energy (eV)

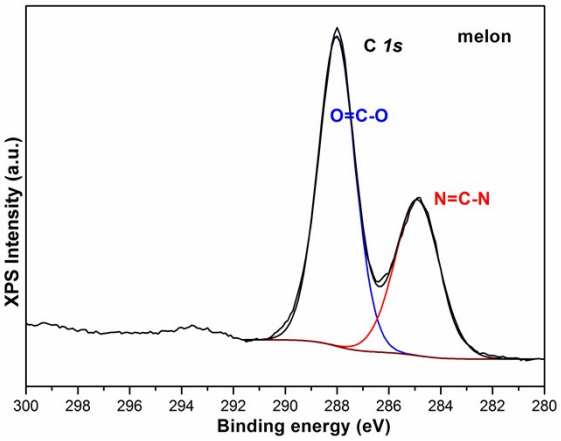
C 1s
melon
O=C-O
N=C-N
XPS Intensity (a.u.)
300
298
296
294
292
290
288
286
284
282
280
Binding energy (eV)

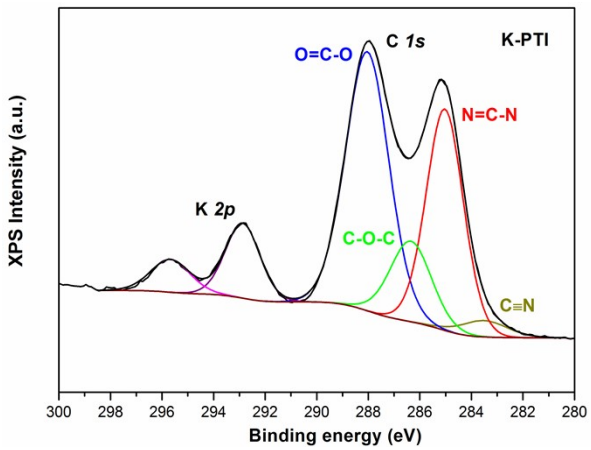
K-PTI
C 1s
O=C-O
N=C-N
K 2p
C-O-C
C≡N
XPS Intensity (a.u.)
300
298
296
294
292
290
288
286
284
282
280
Binding energy (eV)

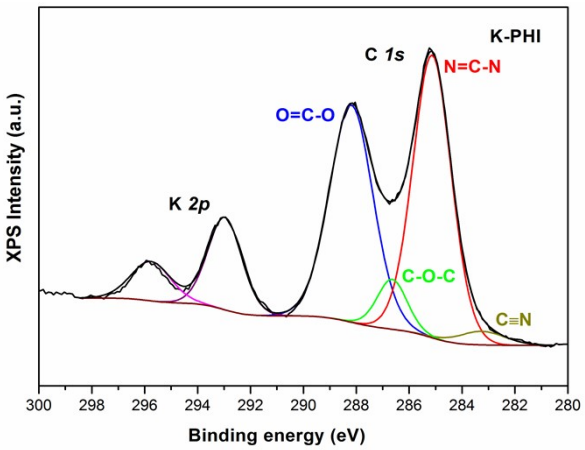
K-PHI
C 1s
N=C-N
O=C-O
K 2p
C-O-C
C≡N
XPS Intensity (a.u.)
300
298
296
294
292
290
288
286
284
282
280
Binding energy (eV)

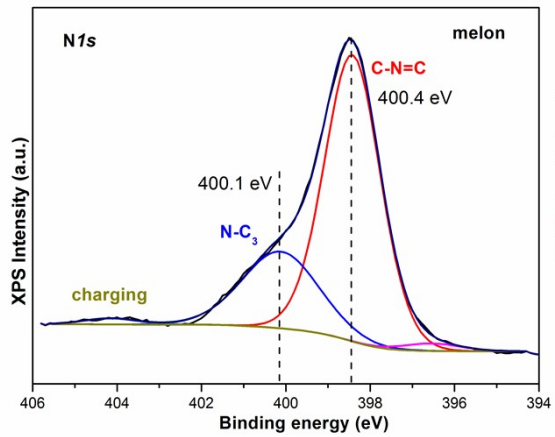
N1s
melon
C-N=C
400.4 eV
400.1 eV
N-C3
charging
XPS Intensity (a.u.)
406
404
402
400
398
396
394
Binding energy (eV)

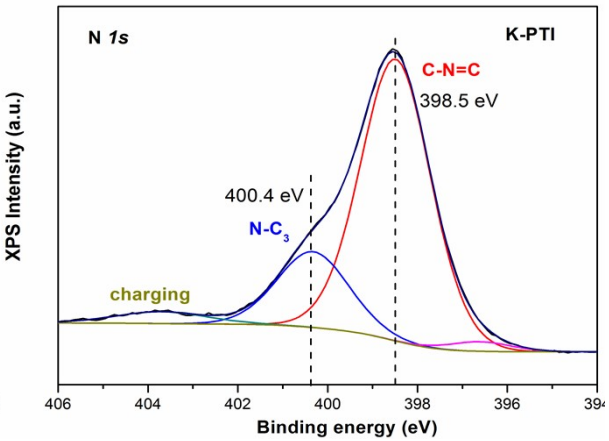
N 1s
K-PTI
C-N=C
398.5 eV
400.4 eV
N-C3
charging
XPS Intensity (a.u.)
406
404
402
400
398
396
394
Binding energy (eV)

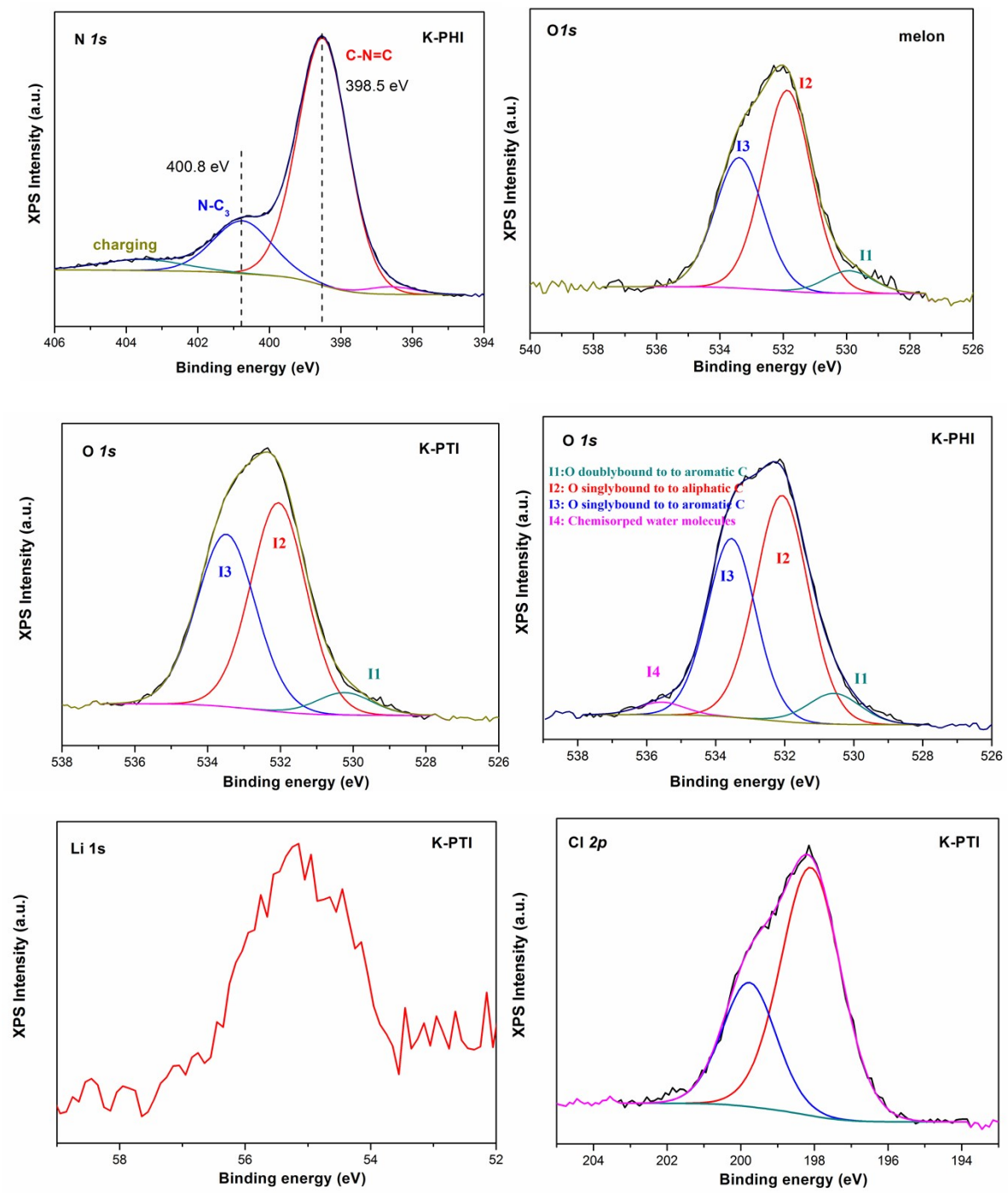

Figure S3. Survey spectra, High-resolution C1s, K2p, N1s, O1s, Li1s and Cl2p XPS analysis of melon, K-PTI and K-PHI photocatalysts as investigated for photocatalytic H_2 evolution studies.

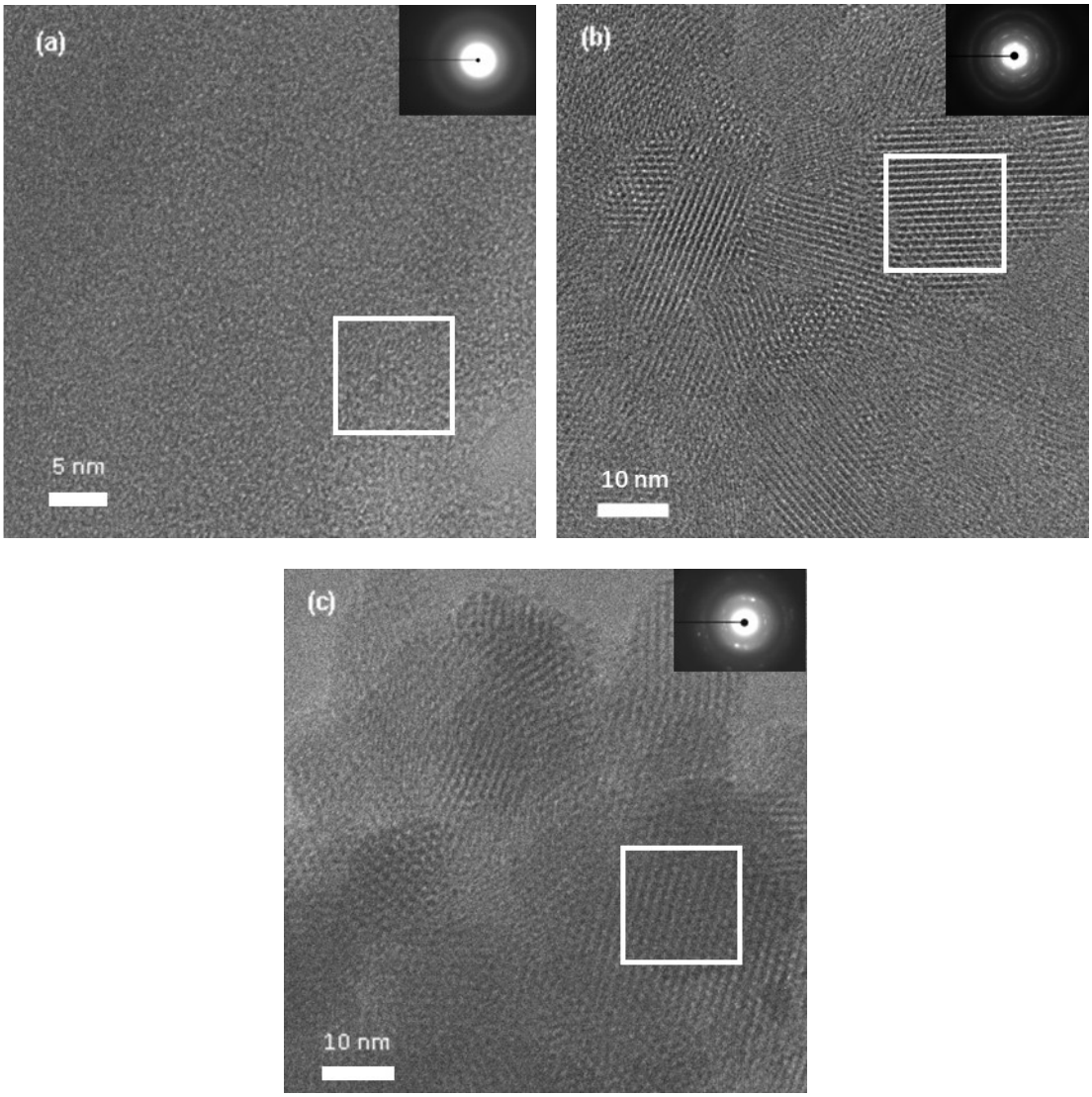

Figure S4. HR-TEM images of different CN photocatalysts as investigated for photocatalytic H_2 evolution studies: (a) melon, (b) K-PHI, (c) K-PTI. Selected are as marked in (a), (b) and (c) were exemplified in Figure 1.

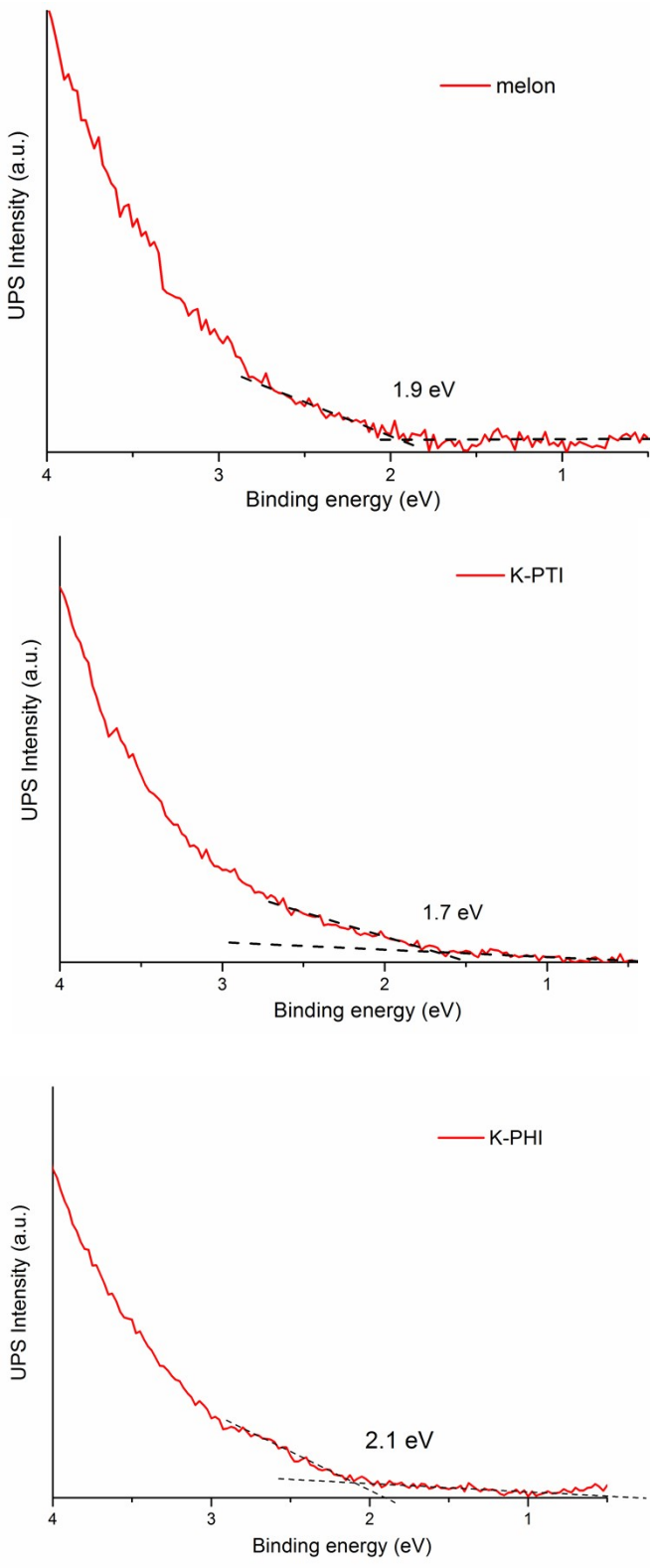

Figure S5. UPS analysis of melon, K-PTI and K-PHI.

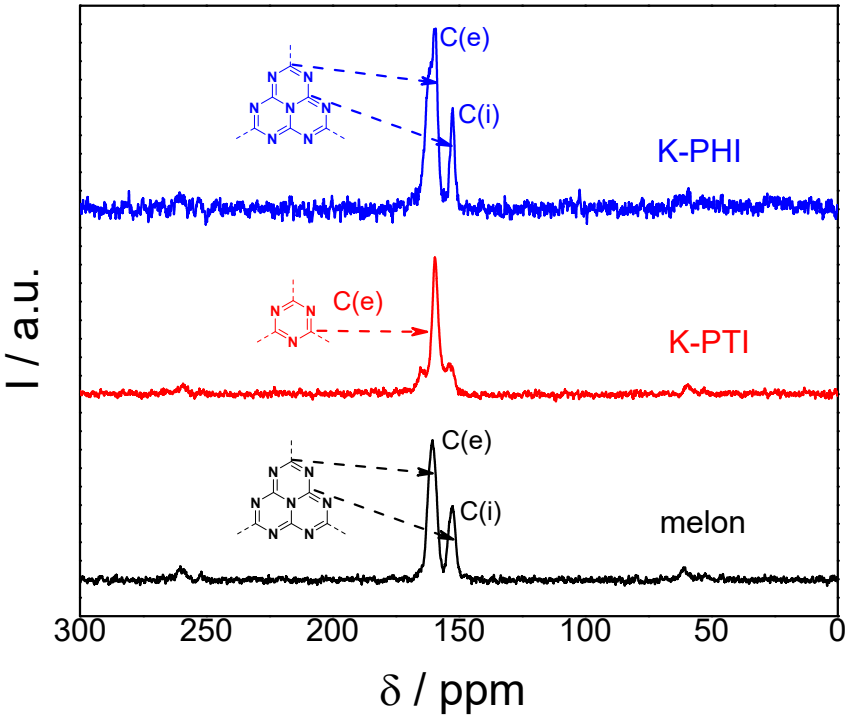

Figure S6. Solid-state C^{13} NMR analysis of melon, K-PTI and K-PHI.

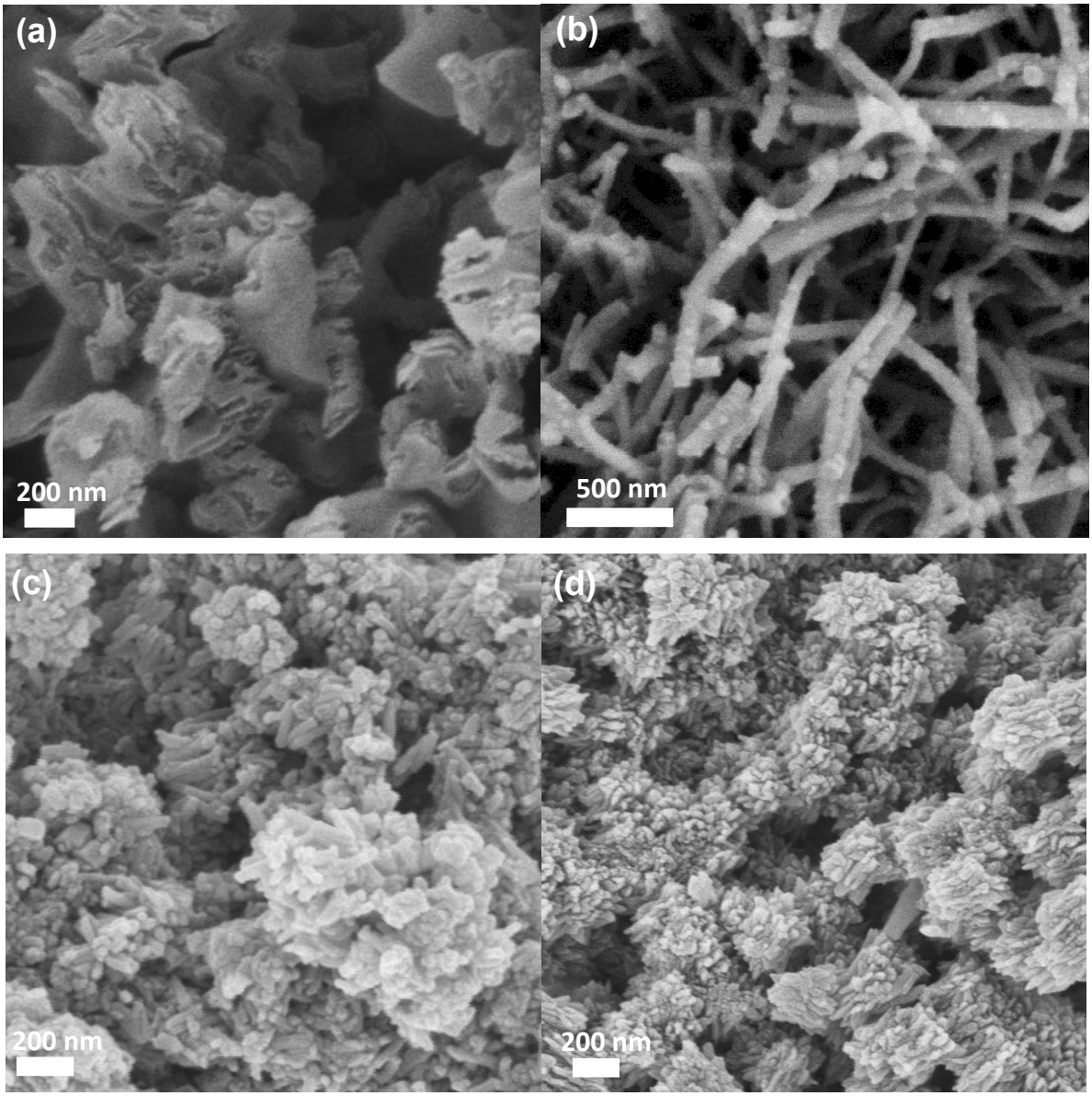

Figure S7. SEM images of different CN photocatalysts as investigated for photocatalytic H_2 evolution studies (a) melon, (b) K-PTI, (c) K-PHI and (d) NaK-PHI.

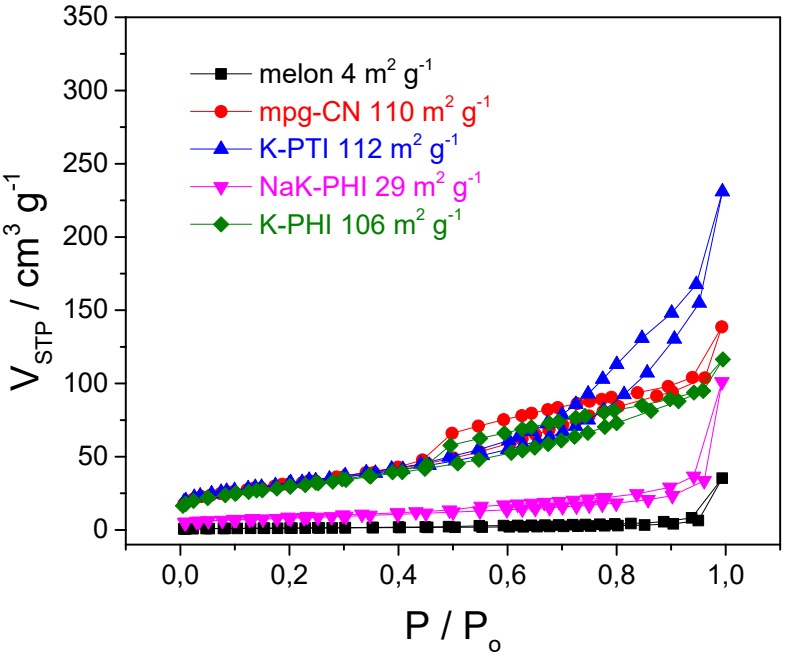

Figure S8. Low temperature (77 K) nitrogen adsorption-desorption isotherms of different CN photocatalysts as investigated for photocatalytic H_2 evolution studies.

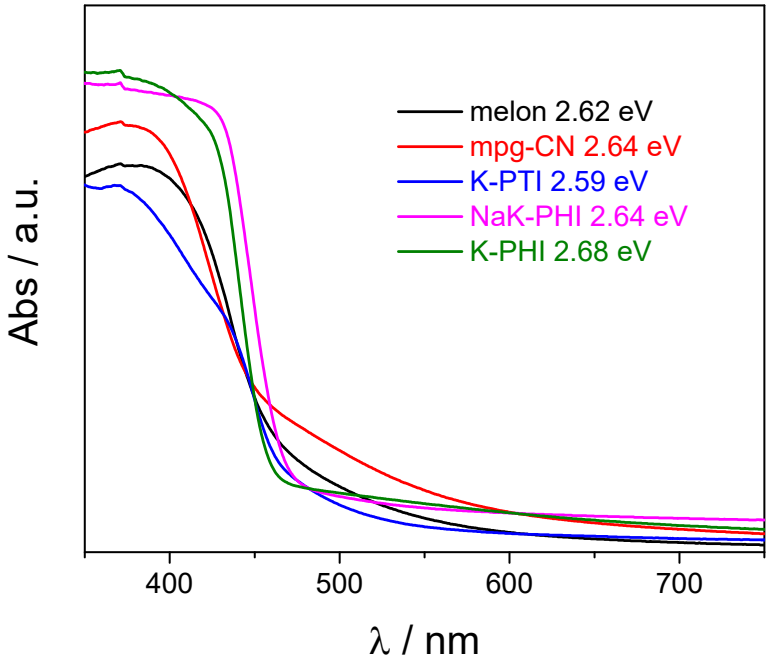

Figure S9. UV-Vis absorption spectra of different CN photocatalysts as investigated for photocatalytic H_2 evolution studies.

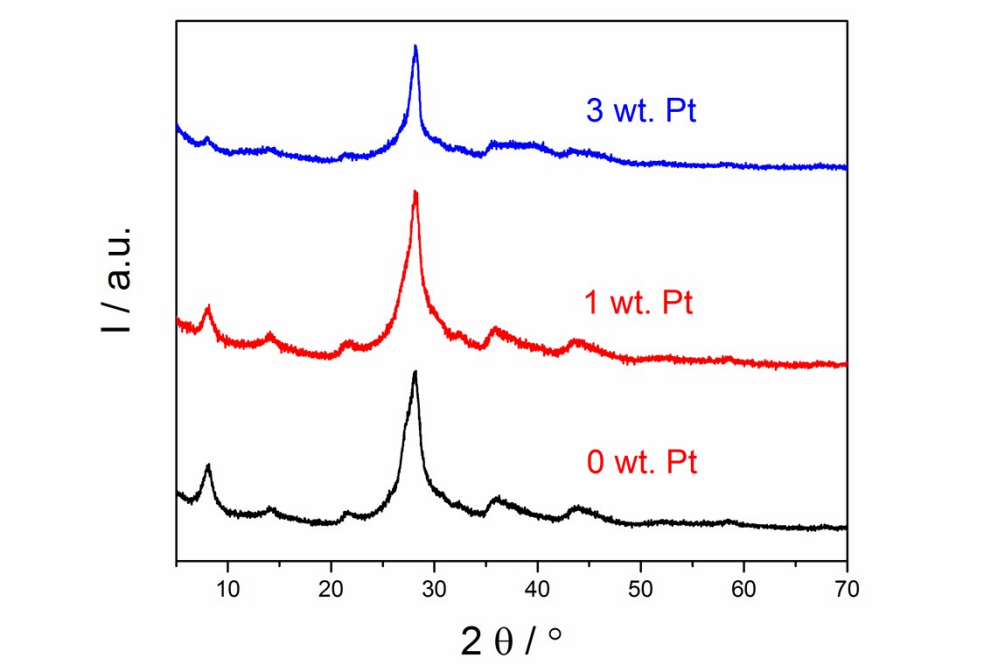

Figure S10. Powder XRD patterns of PtNPs/K-PHI with different Pt loading contents: 0 wt. %, 1 wt. %, and 3 wt. %.

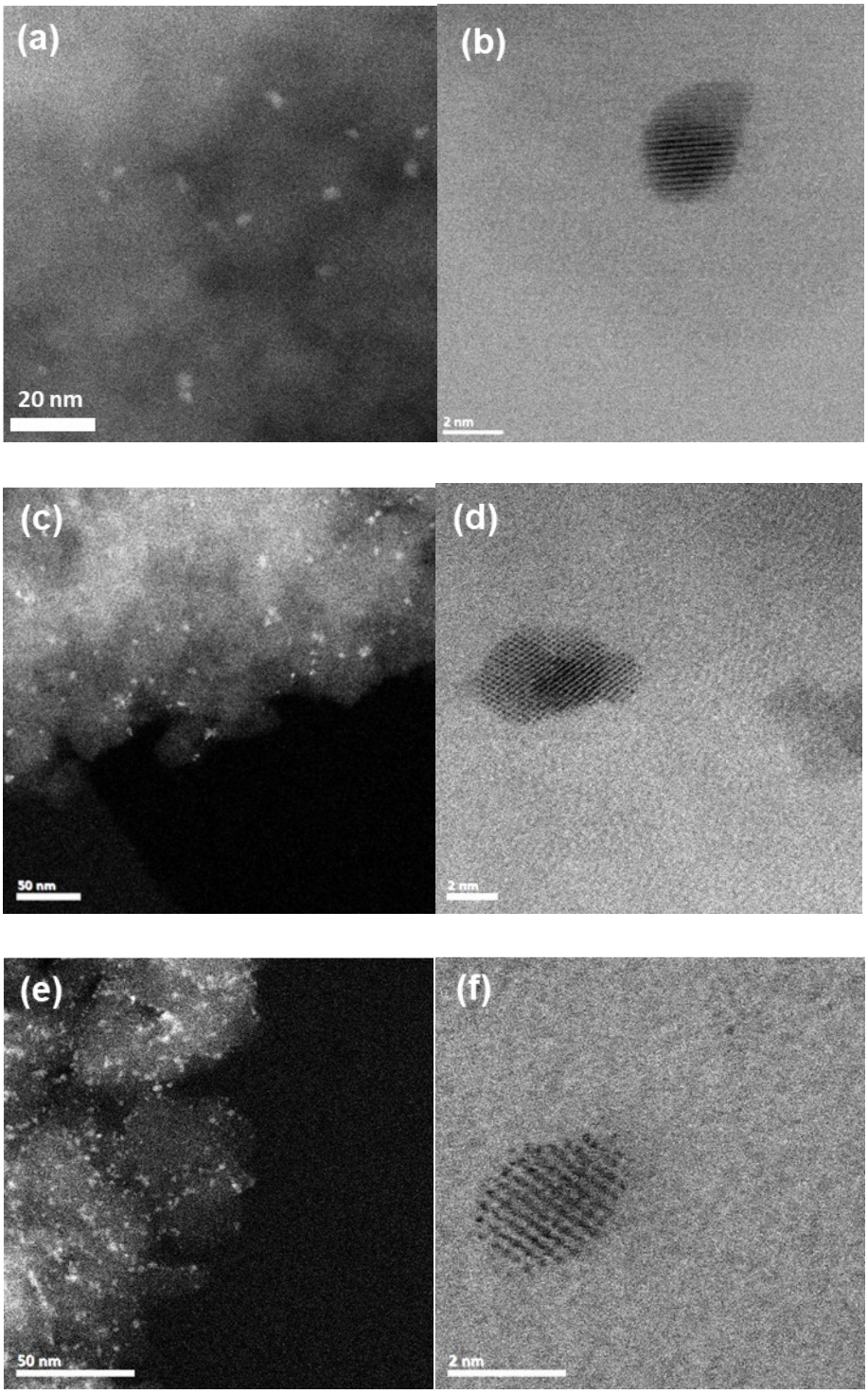

Figure S11. Dark-field scanning transmission electron microscopy (STEM) of PtNPs/K-PHI with different Pt loading contents: 0.1 wt.% (a) and (b), 0.5 wt. % (c)and (d), and 3 wt. % (e) and (f).

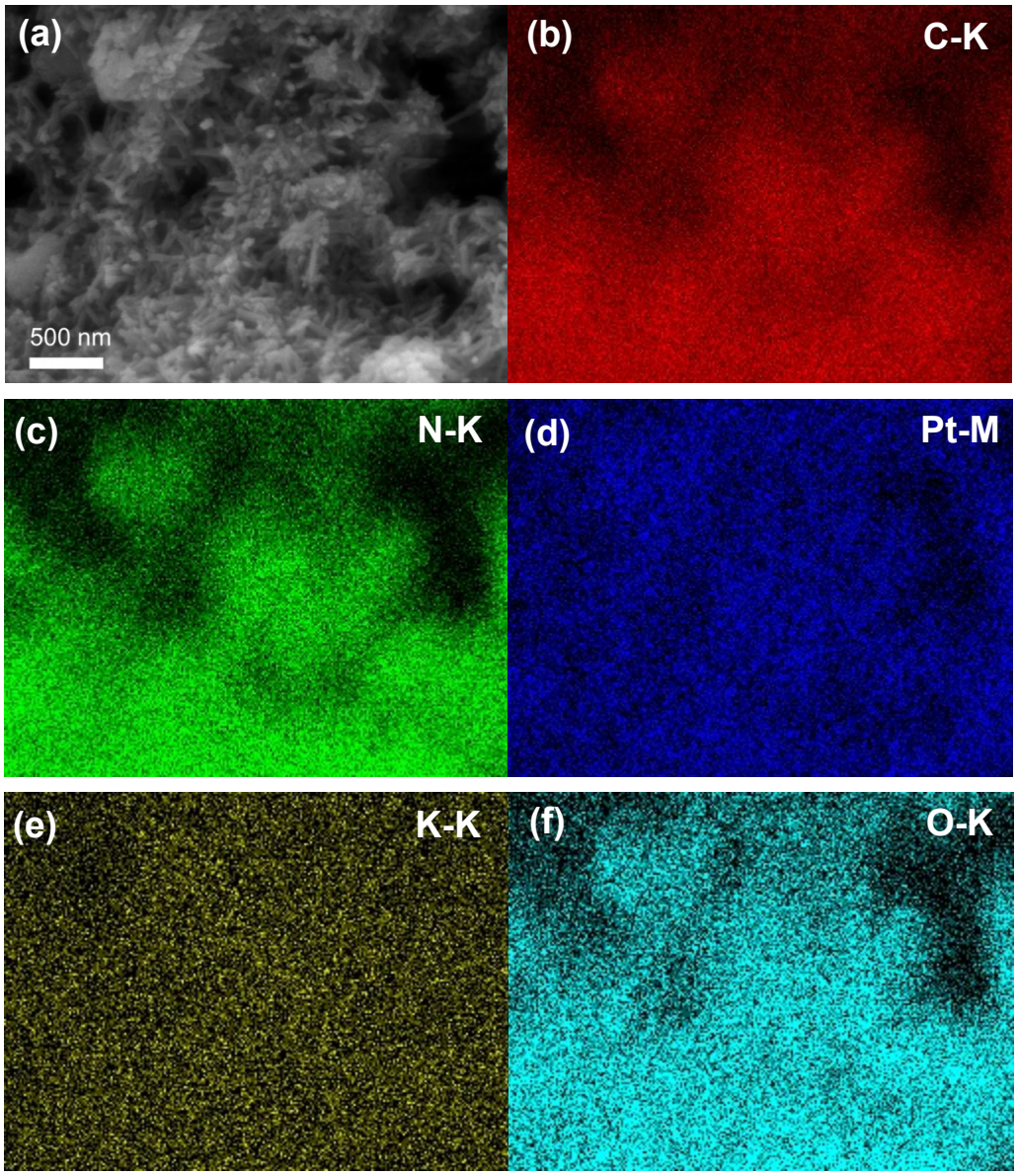

Figure S12. Scanning electron microscopy (SEM) image (a) and (b-f) corresponding elemental mappings recorded for the as-prepared PtNPs/K-PHI sample.

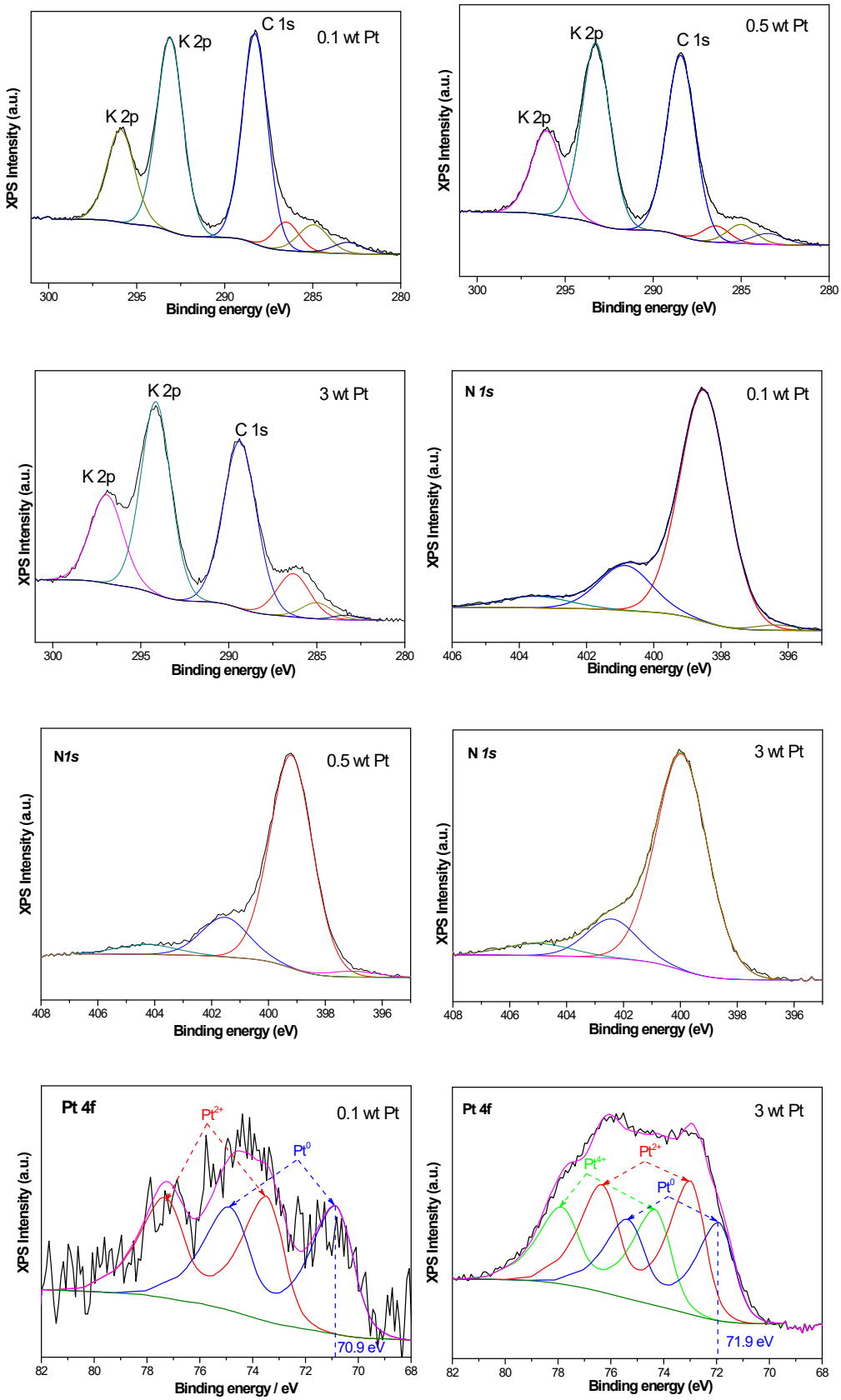

Figure S13. High resolution XPS analysis of PtNPs/K-PHI with different Pt loading contents: 0.1 wt. %, 0.5 wt. %, and 3 wt. %.

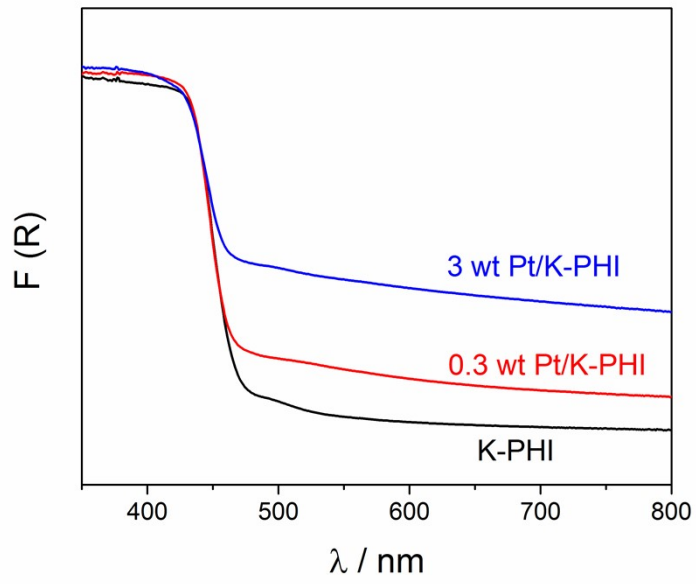

Figure S14. Powder XRD patterns of PtNPs/K-PHI with different Pt loading contents: 0 wt. %, 1 wt. %, and 3 wt. %.

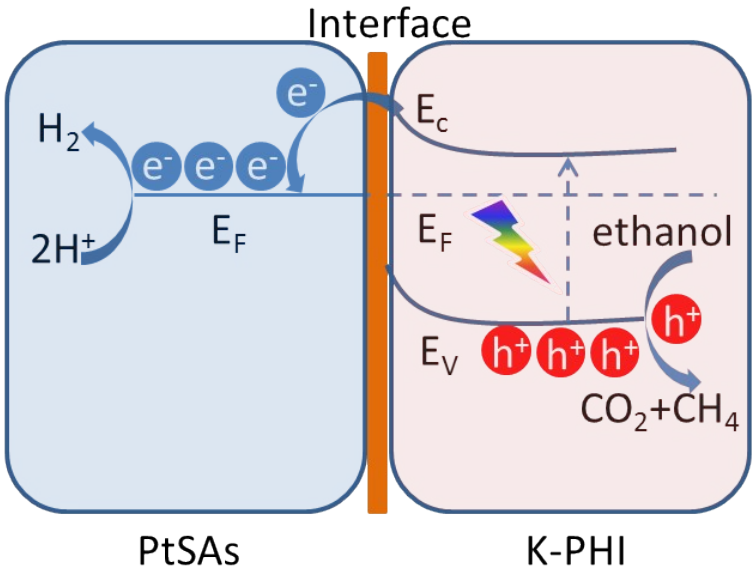

Figure S15. Proposed reaction scheme of photocatalytic H_2 production from reforming of biomass derivatives catalyzed by PtNPs anchored on K-PHI.

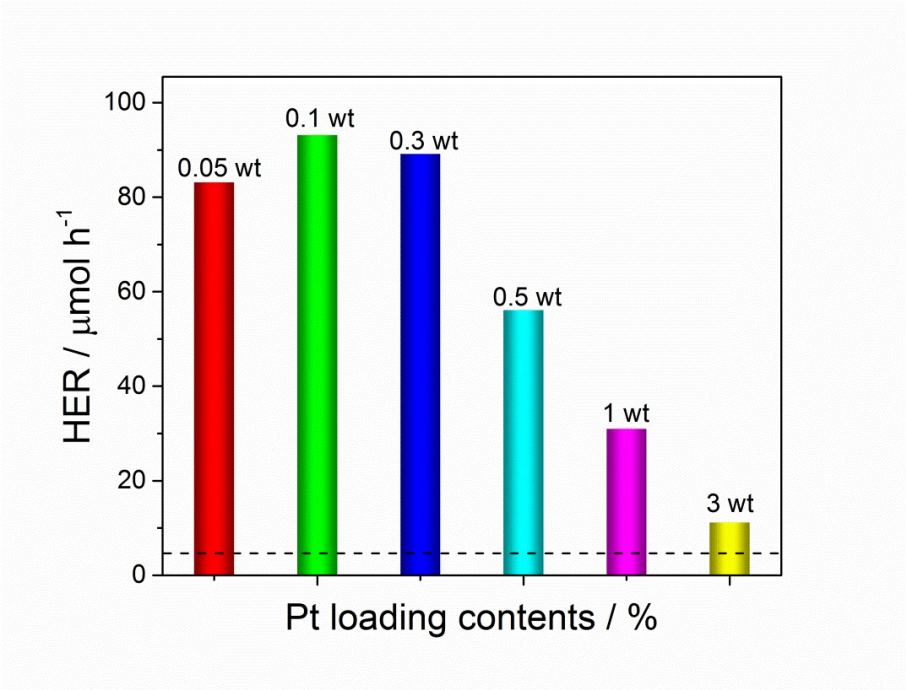

Figure S16. Photocatalytic H_2 evolution by K-PHI deposited with different amounts of Pt from water and ethanol mixture under visible light irradiation.

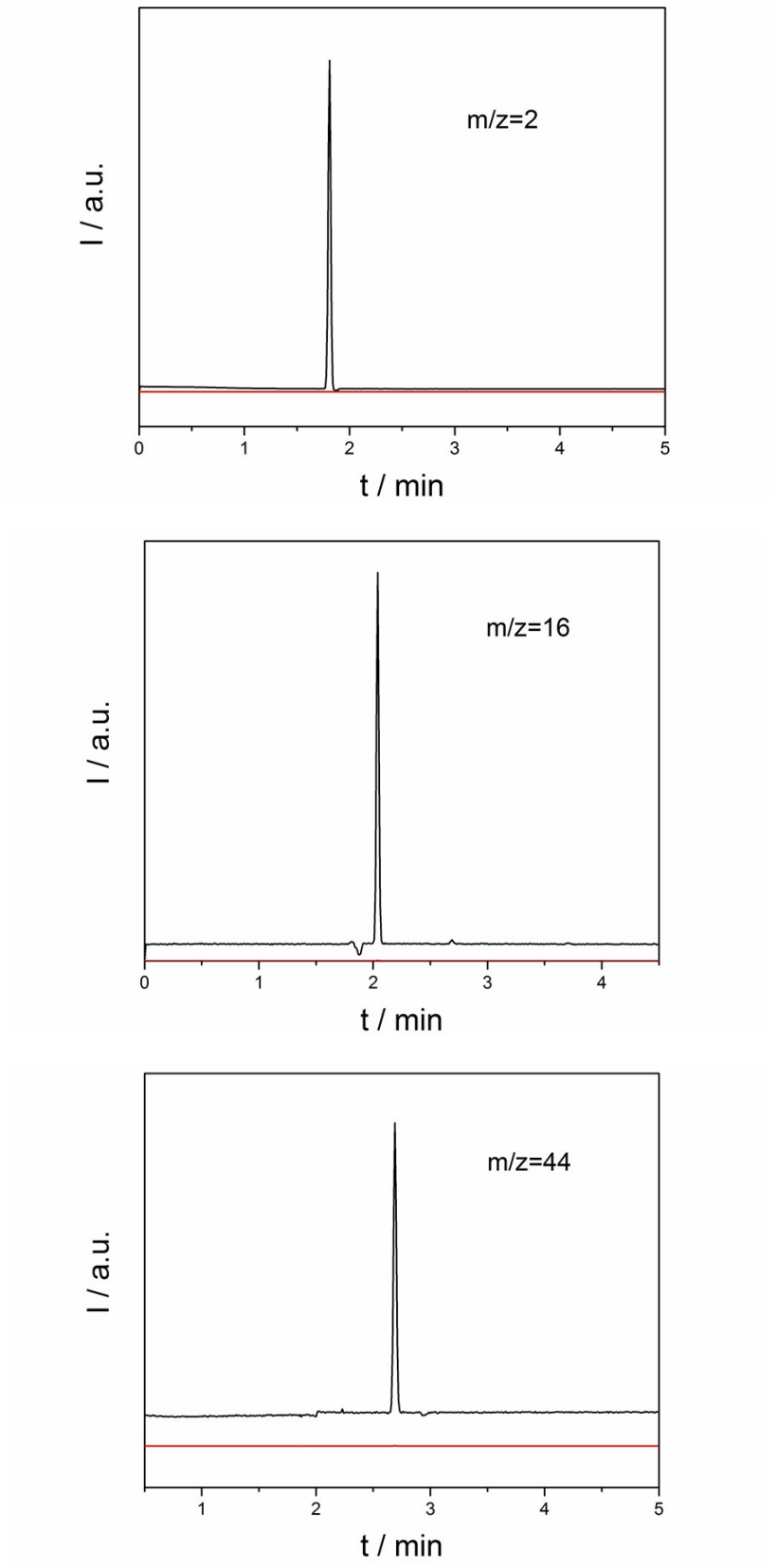

Figure S17. GC-MS analysis of the gaseous products (m/z=2 H_2, m/z=16 CH_4, and m/z=44 CO_2) collected after photocatalytic reforming of ethanol catalyzed by PtNPs/K-PHI.

melon

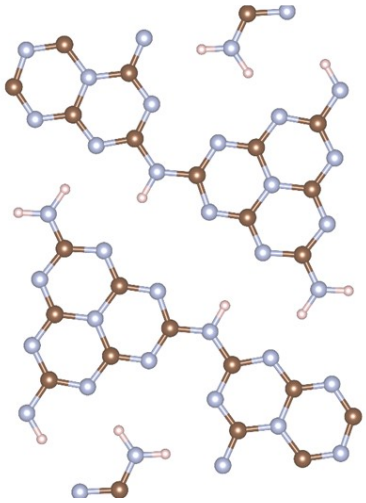

Pt/melon

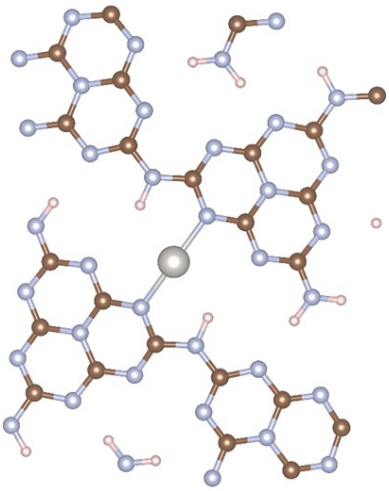

H-adsorption

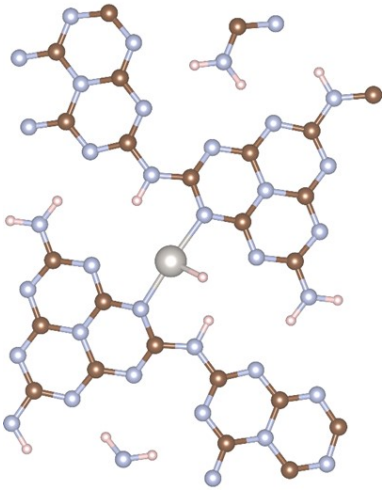

H_2O-adsorption

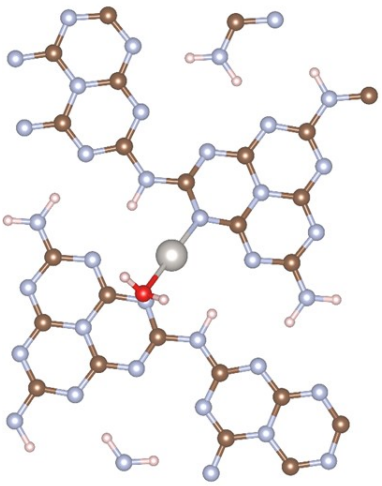

TS

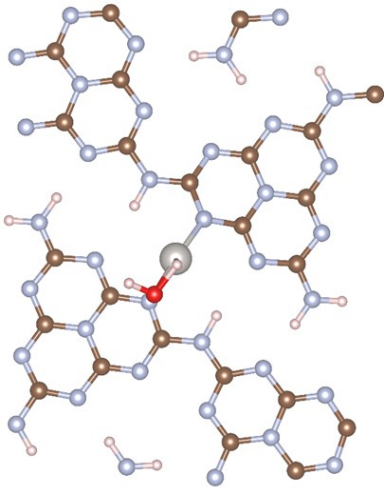

H and OH co-adsorption

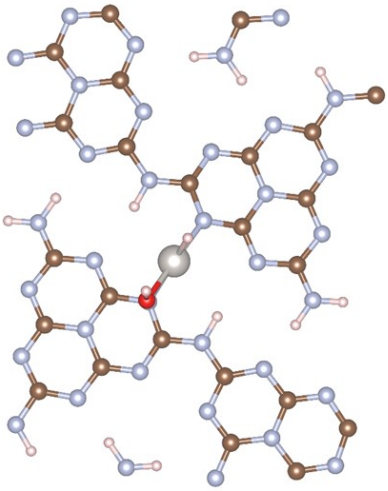

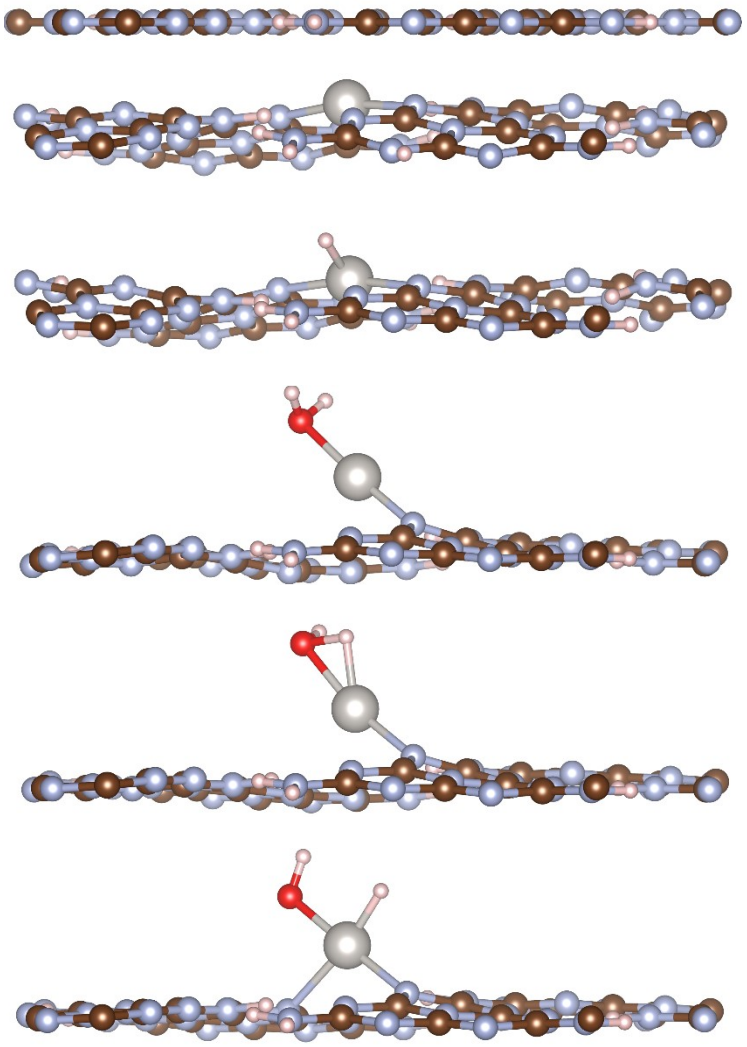

K-PHI

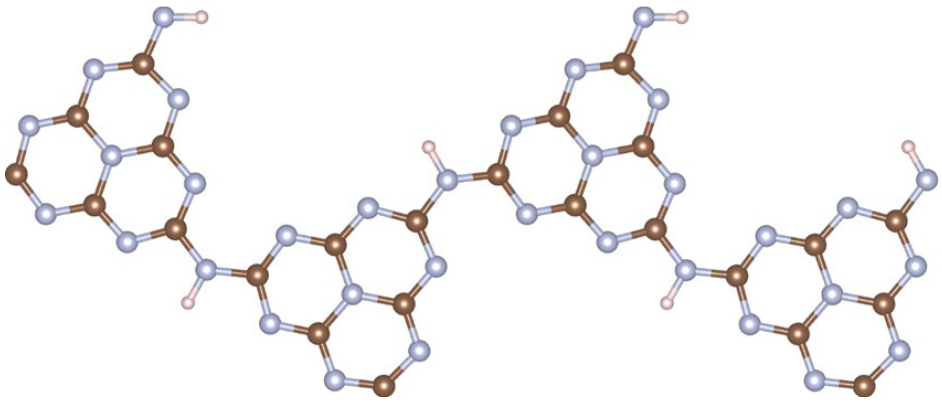

Pt/K-PHI

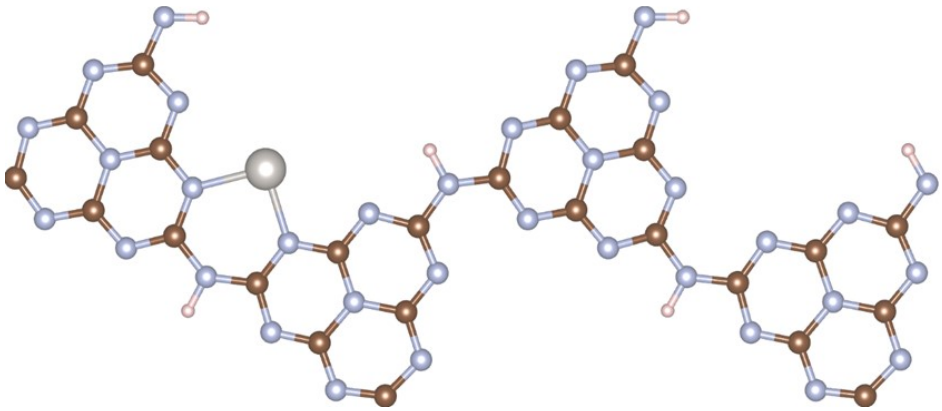

H-adsorption

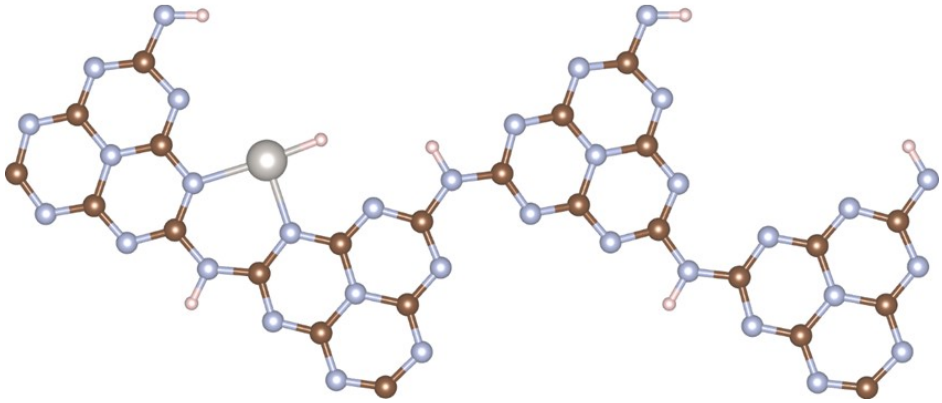

H_2O-adsorption

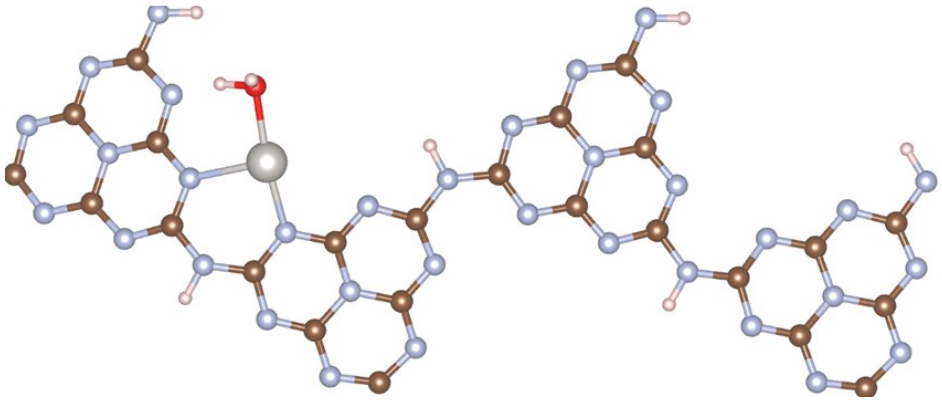

TS

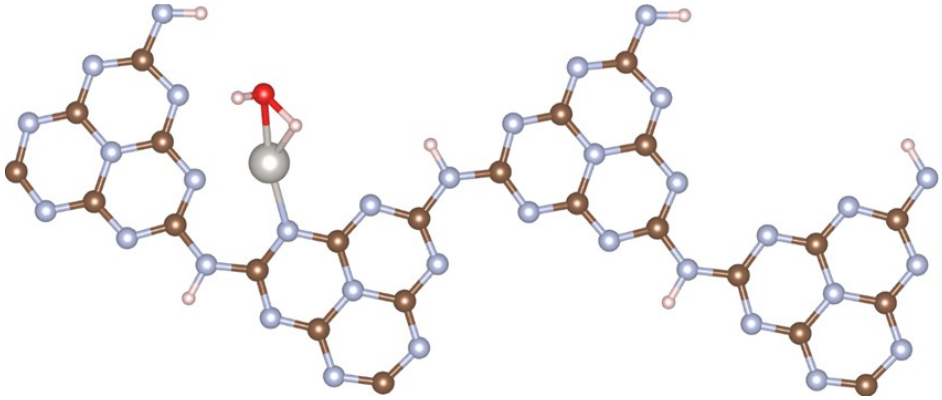

H and OH co-adsorption

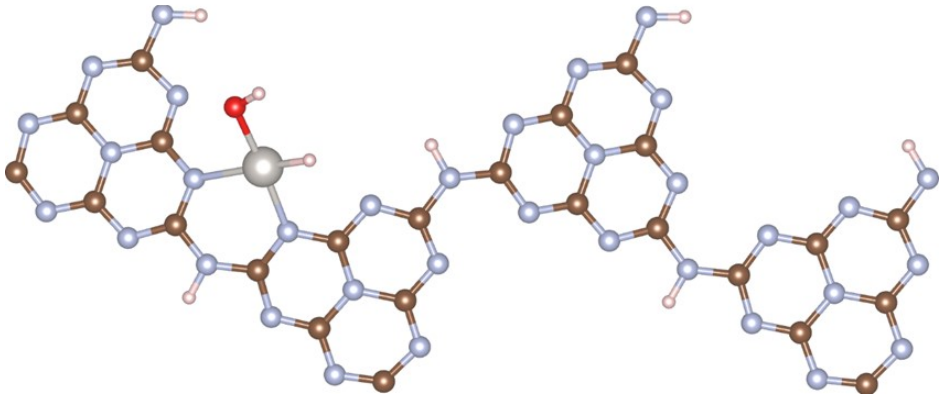

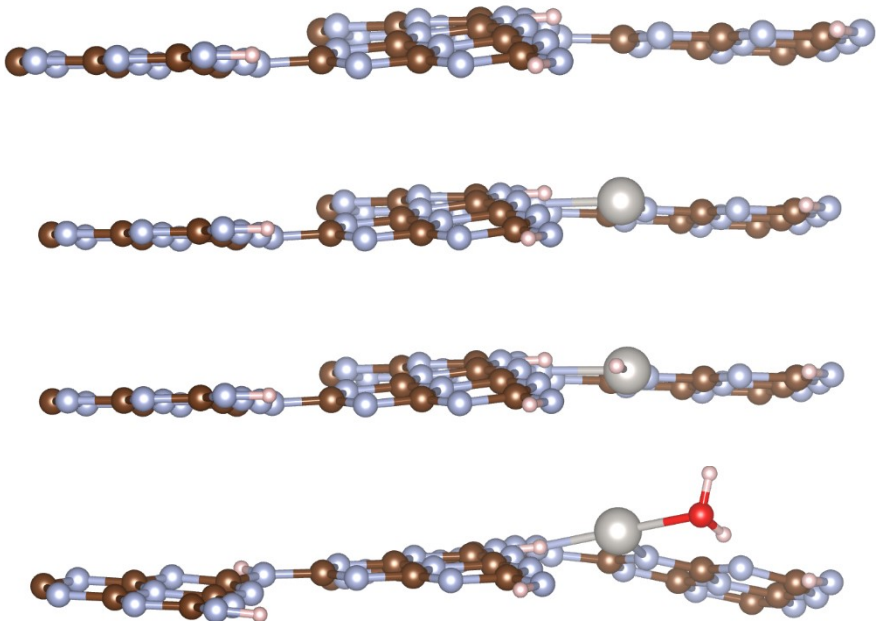

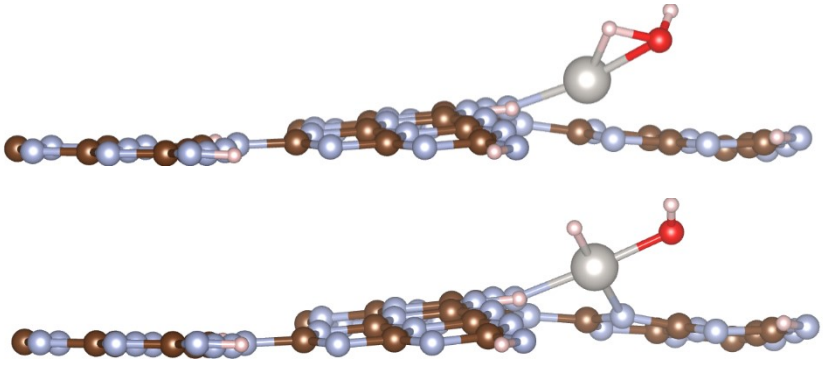

K-PTI

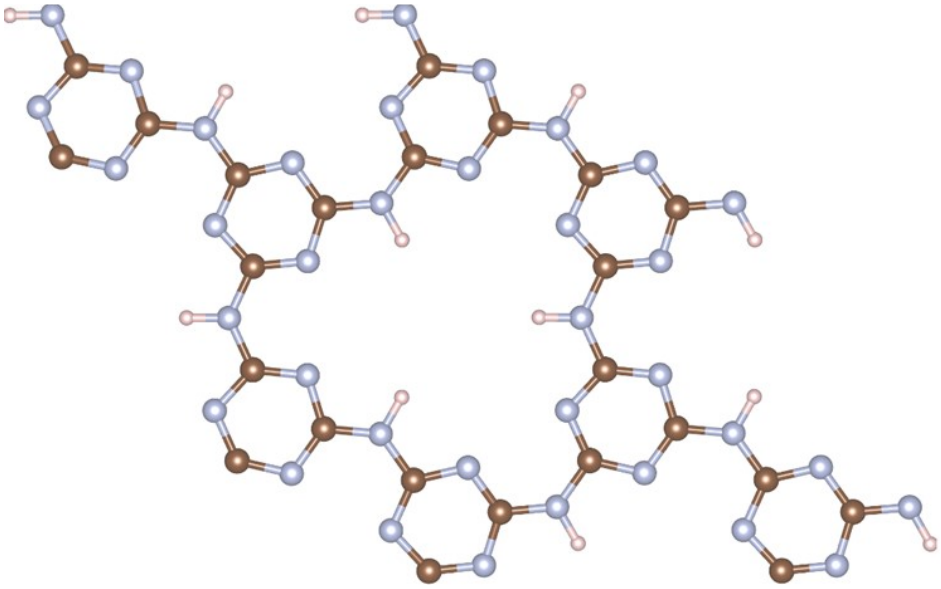

Pt/K-PTI

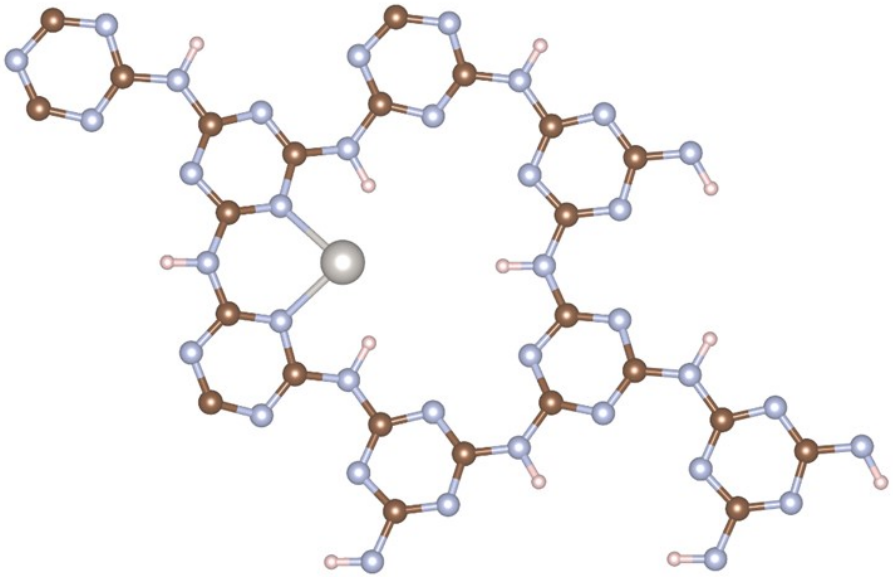

H-adsorption

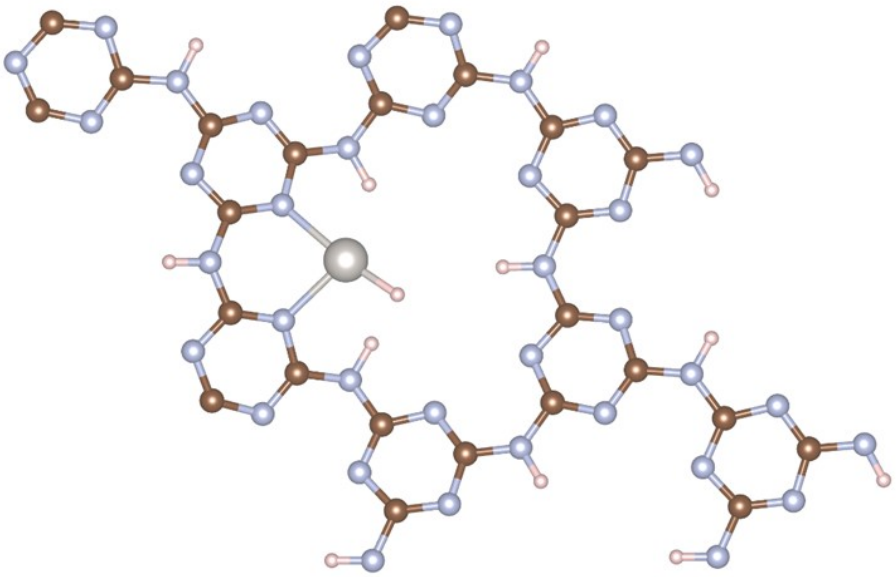

H_2O-adsorption

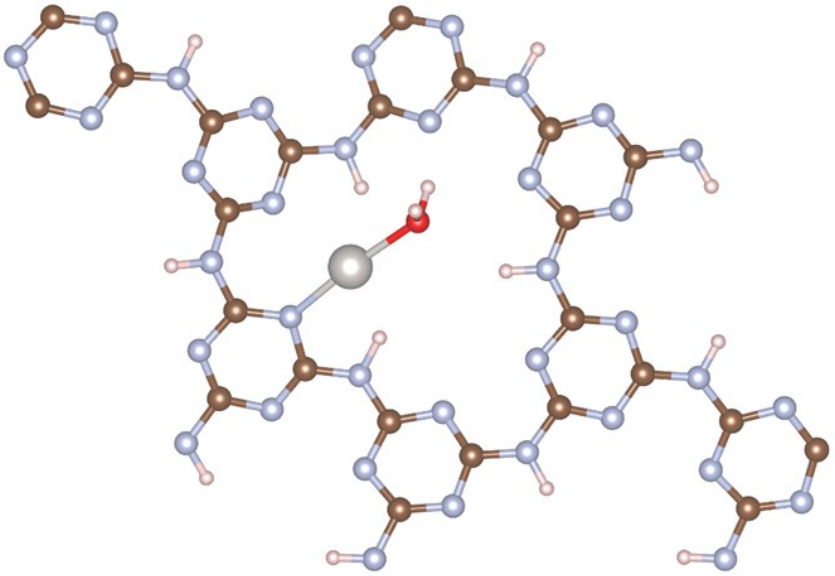

TS

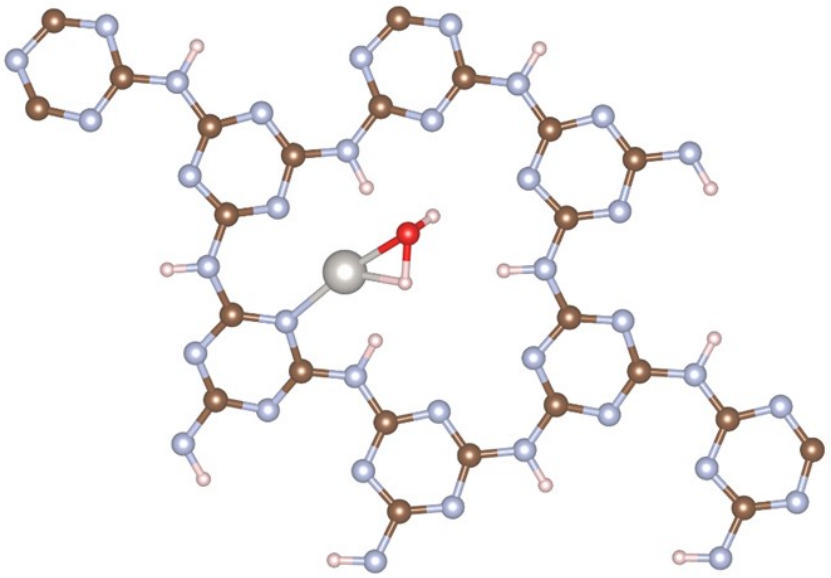

H and OH co-adsorption

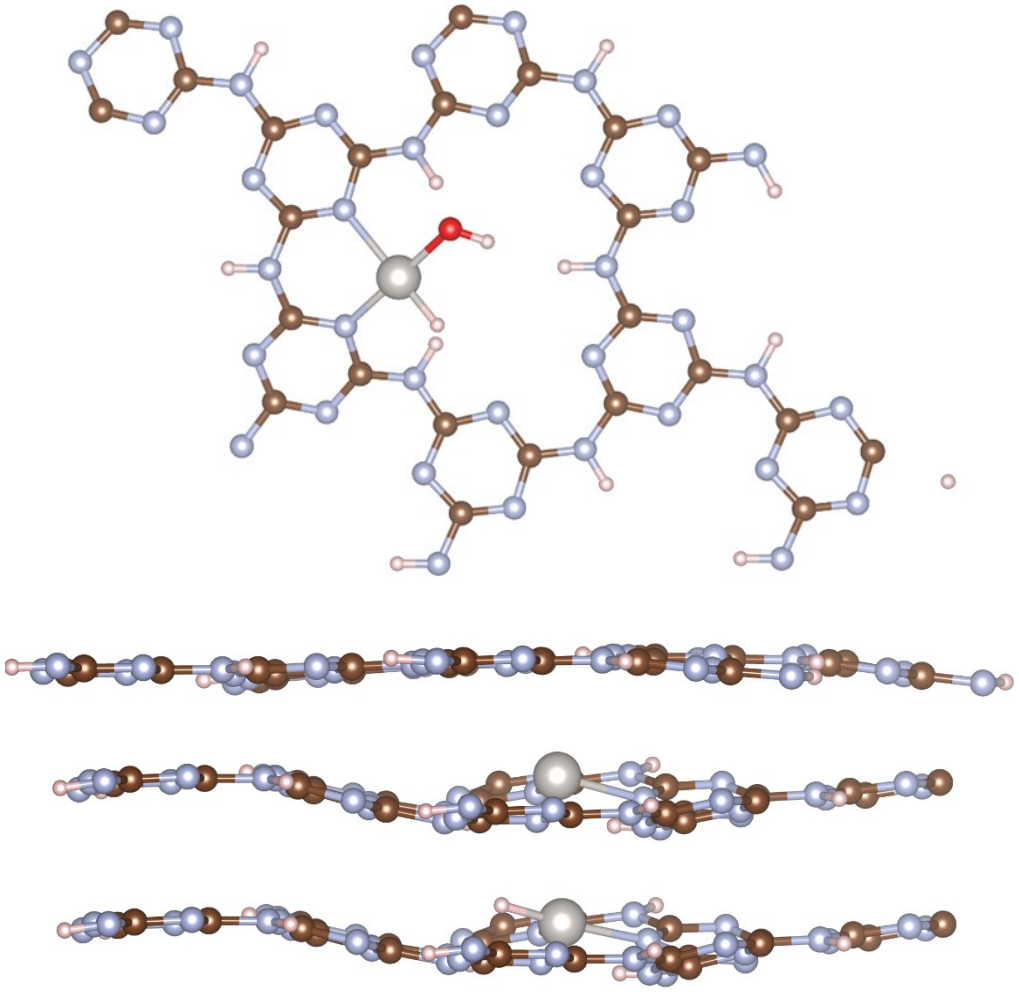

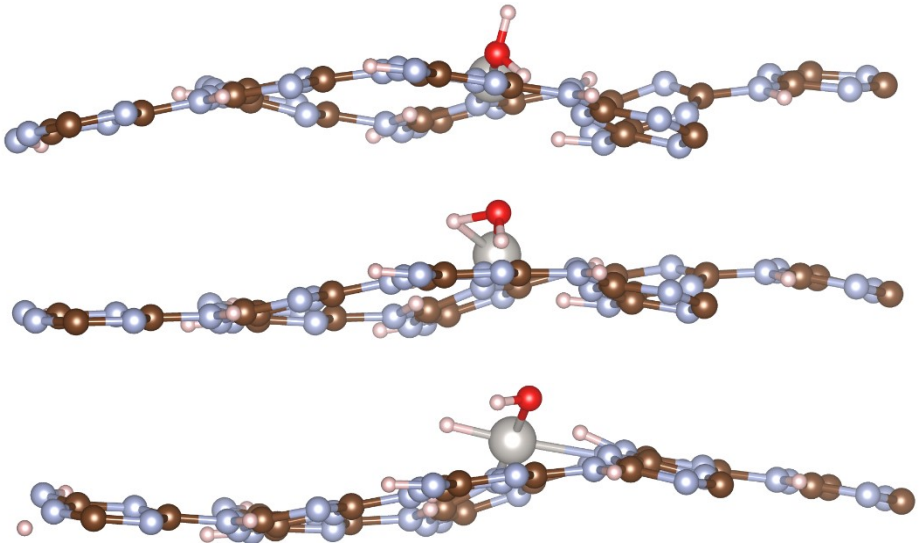

Figure S18. The top and the side view of the most stable structure of melon, K-PHI, K-PTI, and their associated adsorption configurations. The red, brown, blue, pink and gray balls represent O, C, N, H and Pt atoms, respectively.

(1) $CH_3CH_2OH + H_2O \xrightarrow{hv,\ PtNPs/K\text{-}PHI} CH_3COOH + H_2$

(2) $CH_3COOH \xrightarrow{hv,\ PtNPs/K\text{-}PHI} CH_4 + CO_2$

overall reaction:

(3) $CH_3CH_2OH + H_2O \xrightarrow{hv,\ PtNPs/K\text{-}PHI} CH_4 + CO_2 + H_2$

Scheme S3. Proposed reaction pathway of photocatalytic reformation of ethanol for H_2 and CH_4 evolution.

Table S1. Surface atomic ratios of all elements measured by XPS.

Sample	C %	N %	O %	K %	Pt %
0.1 wt. Pt/K-PHI	37.7	46.25	7.4	8.63	0.02
0.5 wt. Pt/K-PHI	38.2	44.8	7.4	9.4	0.2
3 wt. Pt/K-PHI	39.5	39.7	10.6	9.3	0.9

Table S2. Fitting results of time-resolved photoluminescence spectra of K-PHI and PtNPs/K-PHI.

Samples	τ_{AV}(ns)	τ_1(ns) (Rel %)	τ_2(ns) (Rel %)
K-PHI	2.67	1.01 (37)	3.29 (73)
PtNPs/K-PHI	1.07	0.74 (63)	3.24 (29)

TableS3. Comparing of the photocatalytic H_2 evolution activities of the materials by reforming of biomass or biomass derivatives in the literatures.

Catalysts	Light	Biomass	HER / μmol h^{-1}	AQY	Ref.
Pt/TiO_2	UV	glucose	200	-	1
$Pt/ZnSn(OH)_6$	high-pressure mercury lamp	ethanol	800	-	2
Pt/CCNNSs	>420 nm	methanol	53	8.57	3
CCN_{550}	>420 nm	methanol	33	6.8	4
CdS/MoS_2	>400 nm	glucose	5500	-	5
$Pt/o\text{-}g\text{-}C_3N_4$	fullarc	glucose	4.6	-	6
$Pt/PdO_2/Cu_2O$	>420 nm	glucose	11.3	-	7
$Pt/Urea\text{-}CN_x$	AM1.5	methanol	56.2	-	8
CdS/PdO_x	AM1.5	lignocellulose	-	1.2	9
$Pt/g\text{-}C_3N_4$–DND	>420 nm	methanol	41.7	6.25	10
PtNPs/K-PHI	420 nm LED	ethanol	93	15	This work

Supplementary References

[1] X. Fu, J. Long, X. Wang, D. Y.C. Leung, Z. Ding, L. Wu, Z. Zhang, Z. Li, X. Fu, Photocatalytic reforming of biomass: A systematic study of hydrogen evolution from glucose solution. Int. J. Hydrog. Energy. 33 (2008) 6484-6491.

[2] X. Fu, D.Y.C. Leung, X. Wang, W. Xue, X. Fu, Photocatalytic reforming of ethanol to H_2 and CH_4 over $ZnSn(OH)_6$ nanocubes. Int. J. Hydrog. Energy. 36 (2011) 1524-1530.

[3] H. Ou, L. Lin, Y. Zheng, P. Yang, Y. Fang, X. Wang, Tri-s-triazine-Based Crystalline Carbon Nitride Nanosheets for an Improved Hydrogen Evolution. Adv. Mater. 29 (2017) 1700008.

[4] L. Lin, W. Ren, C. Wang, A. M. Asiri, J. Zhang, X. Wang, Crystalline carbon nitride semiconductors prepared at different temperatures for photocatalytic hydrogen production. ApplCatal B-Environ. 231 (2018) 234-241.

[5] C. Li, H. Wang, J. Ming, M. Liu, P. Fang, Hydrogen generation by photocatalytic reforming of glucose with heterostructured CdS/MoS_2 composites under visible light irradiation. Int. J. Hydrog. Energy. 42 (2017) 16968-16978.

[6] A. Speltini, A. Scalabrini, F. Maraschi, M. Sturini, A. Pisanu,Malavasi, L.,Profumo, A., Improved photocatalytic H2 production assisted byaqueous glucose biomass by oxidized g-C_3N_4. Int. J. Hydrog. Energy. 43 (2018) 14925-14933.

[7] L. Zhang, J. Shi, M. Liu, D. Jing, L. Guo, Photocatalytic reforming of glucose under visiblelight over morphology controlled Cu_2O: efficient charge separation by crystal facet engineering. Chem. Commun. 50 (2014) 192-194.

[8] V. W. Lau, V. W. Yu, F. Ehrat, T. Botari, I. Moudrakovski, T. Simon, V. Duppel, E. Medina, J. K. Stolarczyk, J. Feldmann, V. Blum, B. V. Lotsch, Urea-Modified Carbon Nitrides: Enhancing Photocatalytic Hydrogen Evolution by Rational Defect Engineering. Adv. Energy Mater. 7 (2017) 1602251.

[9] D. W. Wakerley, M. F. Kuehnel, K. L. Orchard, K. H. Ly, T. E. Rosser, E. Reisner, Solar-driven reforming of lignocellulose to H_2 with a CdS/CdOx photocatalyst. Nat. Energy. 2 (2017) 17021-17029.

[10] Y. A. Haleem, Q. He, D. Liu, C. Wang, W. Xu, W. Gan, Y. Zhou, C. Wu, Y. Ding, L. Song, Facile synthesis of mesoporous detonation nanodiamond-modified layers of graphitic carbon nitride as photocatalysts for the hydrogen evolution reaction. RSC Adv. 7 (2017) 15390-15396.